1-1-2008

Study on a magnetorheological fluid bladder spring for isolation system

Xianzhou Zhang
University of Wollongong, xianzhou@uow.edu.au

Weihua Li
University of Wollongong, weihuali@uow.edu.au

Xingyu Wang
University of Wollongong

Study on a Magnetorheological fluid bladder spring for isolation system

X.Z. Zhang, W.H. Li*, & X.Y. Wang
School of Mechanical, Materials & Mechatronic Engineering, University of Wollongong, Wollongong, Northfields Avenue, NSW 2522, Australia

ABSTRACT: This paper presents development of a magnetorheological (MR) fluid bladder spring for suppression of vibrations. The developed MR fluid bladder spring is composed of two variable volume rubber bladder filled with MR fluid, a pipe and a MR valve connecting them. One of the bladders supports disturbance force and the MR fluid flows between two bladders because of the variation of bladder volume due to deformation. The shear stress of the MR fluid in MR valve is varied by an applied magnetic field, which thereby varies the characteristics of the isolator, such as its stiffness and damping. A mathematical model of the isolator was derived, and a prototype of the MR fluid bladder spring was fabricated and its dynamic behavior was measured in vibration force for a wide range of frequencies under various applied magnetic fields. The parameters of the model under various magnetic fields were calculated and the bladder dynamic performances were evaluated. A non-resonant control was employed to minimize the vibration amplitude of the system. Numerical simulation results indicated that the semiactive control system produced much better isolation performance than a passive system.

Keywords: Magnetorheological (MR) fluid, bladder, MR valve, isolator, no-resonant control.

1 INTRODUCTION

Vibration reduction and isolation plays an important role in protecting machinery and structures from unwanted vibration related problems. In general, the problem of vibration propagation is tackled by isolating the source by mounting the machinery or sensitive equipment on a suspension system. Many vibration isolation devices were developed for the purposes mentioned above. Sun et al. developed a vibration isolation device to protect process and measurement devices in electronic and semiconductor industry from the micro vibration of environment (Sun et al. 2006). Ohta et al. developed a vibration isolating mount device for limiting oscillation in a rolling direction of the power plant mounted on a vehicle (Ohta et al. 2006). Nemoto et al. applied a patent about an active vibration isolation support system for isolating the vibration generated by an engine from the body of vehicle (Nemoto 2006).

Many efforts were done to make the suspension system work in an optimal condition by optimizing the parameters of the suspension system. Sun et al. utilized genetic algorithm to optimize the design parameters of vehicle suspension (Sun et al. 2007). However, for intrinsic limitation of passive suspension system the improvement is effective only in a certain frequency range, because passive design for low frequency is difficult and often represents a compromise between isolation performance and the supported machinery alignment (Daley et al. 2006).

Compared with passive suspensions, active suspensions can improve the performance of the suspension system over a wide range of frequency. Daley et al. investigated the "smart spring" mount by using a hybrid active/passive method (Daley et al. 2006). Cronje et al. developed a variable stiffness and damping tunable vibration isolator with a closed-loop displacement and velocity feedback control system (Cronje et al. 2005). Zhu et al. (2006) proposed an active acceleration control scheme to control the microgravity vibration isolation systems. Anakwa et al. (2002) developed and controlled a prototype pneumatic active suspension system, which used a pneumatic actuator for active damping. However, active vibration isolation systems are less commonly used than passive systems due to their associated cost, power requirements and fail-safe problems.

Semi-active suspensions can be nearly as effective as fully active suspensions in vibration suppression. Furthermore, they do not require either higher-

power actuators or a large power supply. When the control system fails, the semi-active suspension can still work in a passive condition. In early semi-active suspension, the tunable damping force can be achieved by using hydraulic semi-active dampers with electromagnetically controlled valves or Friction damper, which damping force is controlled by varying the force normal to a friction interface. More recently, the applications of MR fluids in the controllable dampers were investigated and used as semi-active structural control devices successfully. Duan et al. (2006) implemented a total of 312 MR dampers (Lord Corporation) in a bridge for control of rain-wind-induced cable vibrations. Spencer et al. (1998) used the same MR damper to study seismic response reduction by carrying out a series of earthquake tests. Their results indicate that the MR damper is quite effective for structural response reduction over a wide class of seismic excitations. Wang (2002) and his group paid attention to enhancing the protection of infrastructure's elements by studying vibration control of a two-span scaled MR damper bridge model. Other MR devices, including brakes, isolators and engine mounts, were designed, manufactured and experimentally evaluated (Li et al. 2003, Choi et al. 2005, 2003).

In this paper, a novel MR fluid bladder isolator is designed and fabricated. A mechanical model for the isolator is constructed and parameters of the model are identified based on the experimental results. A non-resonant control is employed to minimize the vibration amplitude of the system. In numerical simulations, the performance of the sweeping frequency response reduction and the displacement transmissibility is investigated.

2 MRF ISOLATOR

2.1 *Schematic of MRF isolator*

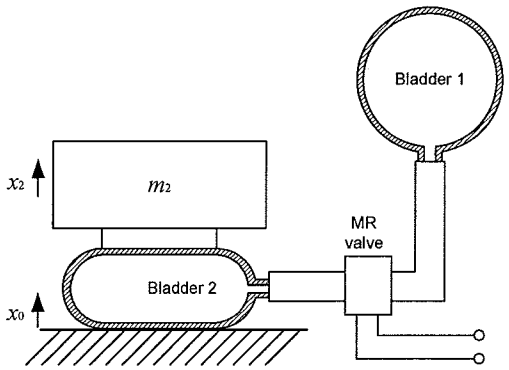

Figure 1. Schematic of the MRF isolator.

The schematic of the developed MRF isolator is shown in figure 1. The proposed isolator is based on a MR fluid bladder spring, which is composed of two variable volume rubber bladders filled with MR fluid, a pipe and a MR valve connecting them. One of the bladders supports a disturbance force and MR fluid flows between two bladders because of the variation of bladder volume due to deformation. The shear stress of the MR fluid in MR valve is varied by the applied magnetic field, which thereby varies the characteristics of the isolator, such as its stiffness and damping.

2.2 *MRF isolator mathematical model*

Figure 2 shows the structure of the vibration isolation systems modeled by the linear springs k_0, k_1 and k_2, the damping factor of the system c_0, c_1. k_0 is the change of area stiffness, which represents the fact that the effective area changes as the bladder is compressed or expanded. k_1 and k_2 are the stiffness of bladder 1 and bladder 2, respectively. The MR damping factor c_1 that can be changed with the magnetic field applied on the MR valve. m_2 is the sprung mass and m_1 is the mass of moving MR fluid. The displacement equation are presented by

$$\begin{aligned} m_2\ddot{x}_2 &= -k_2(x_2 - x_1) - k_0(x_2 - x_0) - c_0(\dot{x}_2 - \dot{x}_0) \\ m_1\ddot{x}_1 &= k_2(x_2 - x_1) + k_1(x_1 - x_0) - c_1(\dot{x}_1 - \dot{x}_0) \end{aligned} \tag{1}$$

where x_0 is the input, x_1, and x_2 are displacements of m_1 and m_2. In this design, k_0 is much less than k_1 and

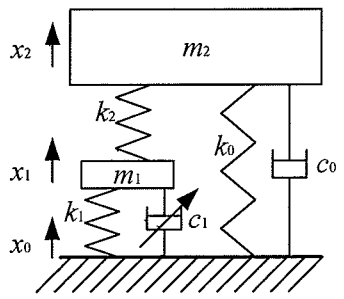

k_2, m_1 is much less than m_2.

Figure 2. The model of the MRE isolator.

Assume initial conditions of both input and output are zeros, the transfer functions is derived as

$$T = \frac{x_2(s)}{x_0(s)} = \frac{c_0 m_1 s^3 + (k_0 m_1 + c_0 c_1)s^2 + (k_0 c_1 + c_0 k_1 + c_0 k_2 + c_1 k_2)s + k_0 k_1 + k_0 k_2 + k_1 k_2}{m_1 m_2 s^4 + (c_0 m_1 + m_2 c_1)s^3 + (m_1 k_0 + m_1 k_2 + m_2 k_1 + m_2 k_2 + c_0 c_1)s^2 + (c_0 k_1 + c_0 k_2 + c_1 k_0 + c_1 k_2)s + k_0 k_1 + k_0 k_2 + k_1 k_2} \tag{2}$$

2.3 *MR valve analysis*

The schematic diagram of the MR valve used in this study is shown in figure 3. The MR valve consists of a C-shaped electromagnet and a fluid gap. The main dimensions of the valve are of L, b and h, where

L = 20 mm, active length of fluid gap
b = 6 mm, active width of fluid gap
h = 4 mm, thickness of fluid gap

The magnetic field produced by a controllable DC power, the inner coil and magnetic pole. In the absence of magnetic fields, the valve produces the damping force only by the fluid-flowing resistance. However, if a magnetic field is supplied to the valve, additional damping force due to the yield stress of the MR fluid would be produced. This damping force of the MR valve can be tuned by changing the applied magnetic field.

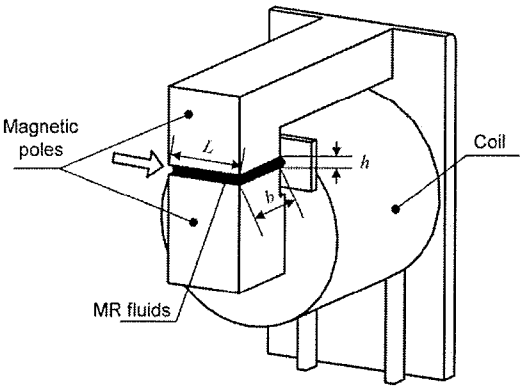

Figure 3. The schematic illustration of MR valve.

Based on the Bingham-plastic flow model, the approximation of the damping force is obtained as follows

$$F = c_{01}\dot{x}_p + F_{MR}\,\mathrm{sgn}(\dot{x}_p) \tag{3}$$

where c_{01} is the viscous damping coefficient without applying magnetic field, which is determined by the plastic viscosity of MR fluids and the geometry of the manufactured damper, F_{MR} is the controllable damping force generated by the applied magnetic field.

For the parallel plate MR value, the damping force is a product of the pressure drop and the effective surface area, given by

$$F = \Delta P \cdot S = \frac{12\eta QL}{bh^3}S = \frac{12\eta LAS}{bh^3}v \tag{4}$$

Here, h is the viscosity of fluid, Q is the volume flow rate, L is the length of fluid gap, b is the width of fluid gap, h is the thickness of fluid gap, A is the section area of MR valve where the fluid flows through, S is effective area causing the pressure of the system (In the case, it is the area of joint between bladder 2 and sprung mass), v is the velocity of fluid at fluid gap of MR valve and F is damping force.

As shown in equation (3), the damping force is due to both viscous effect and MR effect. So the effective viscosity can be represented as

$$\eta_{eff} = \eta_{vis} + \eta_{MR} \tag{5}$$

where $\eta_{vis} = 0.05Pa \cdot s$ is the viscosity of MR fluid without applying magnetic field; η_{MR} is the viscosity increment of MR fluid due to MR effect.

Assuming that MR fluid is incompressible, so the volume flow rate Q is uniform through the whole system. Namely, the volume flow rate generated by sprung mass pressing in bladder 2, $Q_{bladder}$, equals to volume flow rate in the valve, Q_{valve}.

$$Q_{bladder} = S \cdot \dot{x}_p \tag{6}$$

where S=3.14×10^{-4} m^2 is the area of joint between bladder 2 and sprung mass. Substituting all parameters and equations (5) and (6) into equation (4), the damping force is given by

$$\begin{aligned} F = \Delta PS &= \frac{12LS^2}{bh^3}(\eta_{vis} + \eta_{MR})\dot{x}_p \\ &= 61.685(\eta_{vis} + \eta_{MR})\dot{x}_p = c_{eff}\dot{x}_p \end{aligned} \tag{7}$$

where c_{eff} is the effective damping ratio of the MR valve, which is represented

$$c_{eff} = 61.685(0.05 + \eta_{MR}) \tag{8}$$

The viscosities of MR fluid at various magnetic fields were measured using a parallel-plate rheometer (MCR 301, Anton Paar Companies, Germany). Both the steady shear flow mode and oscillatory shear mode (Li et al. 2004) were employed to test the MR sample. Figure 4 shows the effective viscosity of the sample at various magnetic flux densities ranging from 0 mT to 100 mT. From this figure, a quadratic function was fitted to approximate the relationship

$$\eta_{MR} = 1270B_g^{\,2} + 78B_g + 0.05 \qquad (B_g \le 0.1T) \tag{9}$$

where B_g is the flux density.

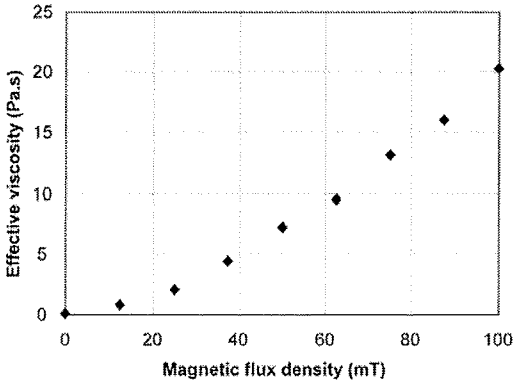

Figure 4. Effective viscosity versus magnetic flux density.

For the developed MR valve, the flux density is proportional to the coil current, which is given by

$$B_g = 0.0432I \qquad (I \le 2.3A) \tag{10}$$

Substitute equations (9) and (10) into equation (8), the damping ratio is rewritten as

$$c_{eff} = 146I^2 + 207I + 3.084 \quad (11)$$

2.4 *Parameter Identification*

From equation (2), the transfer function can be represented in terms of amplitude and phase angel

$$T = \sqrt{\frac{(ac+bd)^2 + (bc-ad)^2}{(c^2+d^2)^2}}$$
$$\theta = \tan^{-1}\left\{\frac{bc-ad}{ac+bd}\right\} \quad (12)$$

where

$$a = k_0k_1 + k_0k_2 + k_1k_2 - (k_0m_1 + c_0c_1)\omega^2$$
$$b = (c_0k_1 + c_0k_2 + c_1k_0 + c_1k_2)\omega - c_0m_1\omega^3$$
$$c = k_0k_1 + k_0k_2 + k_1k_2 - (m_2k_1 + m_1k_2 + m_2k_2 + m_1k_0 + c_0c_1)\omega^2 + m_1m_2\omega^4$$
$$d = (c_0k_1 + c_0k_2 + c_1k_0 + c_1k_2)\omega - (m_1c_0 + m_2c_1)\omega^3$$

As shown in equation (12), if the transmissibility and phase angle are experimentally obtained, the stiffness and damping ratio of the springs can be worked out.

The schematic of the experimental setup is shown in figure 5. The isolator is fixed on an exciter and it is forced to vibrate by the vibration exciter (Type: JZK-5, SINOCERA PIEZOTRONICS, INC. China), which is driven by a signal source from a power amplifier (YE5871-100W) whose signal is provided by the Data Acquisition (DAQ) board (Type: LabVIEW PCI-6221, National Instruments Corporation. U.S.A) and computer. Accelerometer (Type: CA-YD-106) 1 and 2 monitor the vibrations of the base and the mass. The signals are amplified by Charge amplifier (YE5851) and processed by DAQ and computer. A GW laboratory DC power supply (Type: GPR-3030D, TECPEL CO., LTD. Taiwan) can adjust the magnetic field intensity of the isolator and change its dynamic performance.

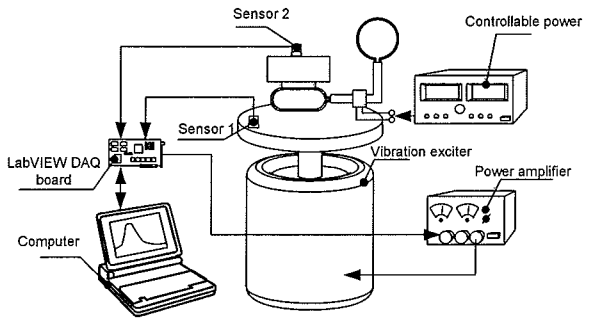

Figure 5. Experimental setup for parameters identification

The testing interface designed in this system acts as the control unit and display unit. The program is designed in LabVIEW (http://www.ni.com/labview/). The essential part of this system is the LabVIEW vibration package, which is used to generate the swept sine signals and to display and record the testing result for the property analysis. It can also be seamlessly connected to equipment PCI6221 DAQ board that are used as the interface between the computer and the amplifiers in this system. This program measures the frequency response of the device with a swept sine technique, generates a tone for the excitation signal and measures the magnitude and phase response of the device. The frequency response is measured at each test frequency, one frequency at a time. This testing program uses two analog input channels and one analog output channel. The start frequency and stop frequency determine the frequency range of the swept-sine measurement. The sample rate is 2.5 times the value of the maximum of the two frequencies.

Figure 6 shows a typical result of the transmissibility and phase versus sweeping frequency. In this experiment, the frequency is swept from 2 Hz to 20 Hz. The number of steps is set as 40, which determines the total number of test frequencies.

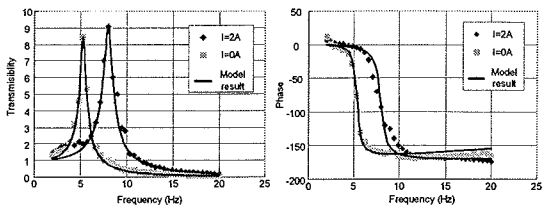

Figure 6 MRF isolator's transmissibility and phase.

Table 1 gives the parameters of the isolator and the experimental results agree with the model results. As can be seen from the figures, the natural frequency of isolator increases from 5.3Hz at without a magnetic field to 8Hz when the current intensity in coil is 2A.

Table 1. Parameters of MRF isolator.

m_1	m_2	k_0	k_1	k_2	c_0	c_1	c_{MR}
0	1kg	0	2000 N/m	2500 N/m	3 Ns/m	3 Ns/m	998 Ns/m

3 SIMULATION EVALUATION

The control strategy based on non-resonance theory was used to control the isolator (Kobori et al. 1993, Pnevmatikos et al. 2004). Kobori described the seismic structural response process using the asymptotic motion equation (Kobori et al. 1993).

$\{\ddot{x}(t)\} = [E(t)](\{SF(t)\} + \{RF(t-\Delta t)\})$

$\{\ddot{x}(t)\}$: seismic structural response

$[E(t)] = f(M(t), C(t), K(t))$: transfer function
$[\mathrm{SF}(t)] = f(M(t), \ddot{y}(t))$: instantaneous seismic force

$$[RF(t-\Delta t)] = f(M(t), C(t), K(t), \ddot{x}(t-\Delta t), \dot{x}(t-\Delta t), x(t-\Delta t)]$$

: instantaneous resonant force (13)

The time-varying transfer function [E(t)] implies the dynamically controllable property in the seismic response control system. This isolator aims to reduce the current response by altering the damping force in [$E(t)$]. That is, to avert resonance under any excitation. By altering its parameters, the system can avoid the build-up of dominant periodic components of excitation. Thus, the input energy to the system and the system response can be reduced. Kobori suggested a control algorithm to shift the building frequencies as far away as possible from the disturbance dominant frequencies. The main idea of the algorithm was that the stiffness of system should be increased if the product of drift $x(t)$ and velocity $\dot{x}(t)$ is positive, that is, if $x(t)$ and $\dot{x}(t)$ are in the same direction. By contrast, if $x(t)$ and $\dot{x}(t)$ are opposite to each other, then the stiffness should be decreased. For this simple control algorithm, the long time calculation of feed back signals can be avoid and the real time control can be obtained easily. In this paper, the control is designed as

$$i(t) = \begin{cases} 1 & x_2(t)\dot{x}_2(t) > 0 \\ 0 & x_2(t)\dot{x}_2(t) \le 0 \end{cases}$$

and $$c_1(t) = \begin{cases} 3 & x_2(t)\dot{x}_2(t) > 0 \\ 1001 & x_2(t)\dot{x}_2(t) \le 0 \end{cases} \quad (14)$$

where $i(t)$ is the control signal.

The diagram of the proposed control system is illustrated in figure 7. The simulink diagram represents the isolator and the lower part in the dash line rectangle represents the controller. This simulation model is based on the displacement equation (equation 1) of the isolator and the controller is based on the non-resonant theory.

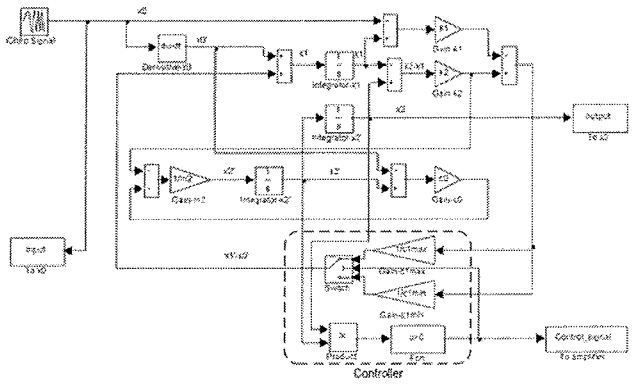

Figure 7. Control system diagram.

Figure 8(a) illustrates the displacement of the excitation signal. The signal is a sine sweeping waves with amplitude 1 from 1 to 15Hz during 15s. Figure 8(b) shows the displacement of the mass m_2 without control. Figure 8(c) shows the vibration amplitude of mass when the MR valve is always working on maximum damping; while Figure 8(d) denotes the response of non-resonant controlled system. It is found that the system without control has a formant frequency and the amplitude is very large when the excitation signal nears this frequency. High damping ratio c_1 can change the original natural frequency of system, but it still resonates at a new natural frequency. It is clear that the amplitude ratio of the non-resonant controlled system is lower than that of the passive system in the whole frequency band, i.e. the controlled MR isolator has a much better isolation effect.

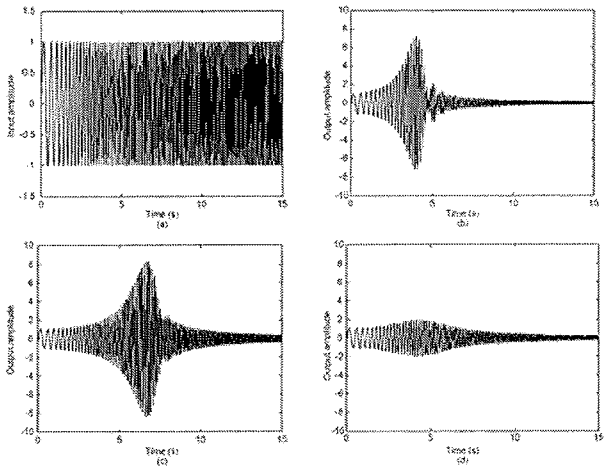

Figure 8. Response signals of the isolation system.

4 CONCLUSIONS

In this paper, a new semi-active vibration isolation system, which is fabricated with rubber bladders and an MR valve, is designed and manufactured. A mathematical model of the MR isolator is built for latter theoretical analysis. To describe the practical damping force generated by the MR valve in the isolator, a numerical model of the MR valve is proposed. Then, using experimental method, the parameters of MR isolator are identified. Meanwhile, dynamic behavior of MR isolator with different excitation frequency and current input is measured and compared with that resulting from theoretical analysis. It was shown that the model calculation result was in sufficiently good agreement with the dynamic properties of the isolator measured from the experiment.

The isolation effect of the MR bladder isolator was evaluated by simulation too. A non-resonant control has been used to minimize the vibration amplitude of the system. The simple controller and quick response of MR valve can provide the isolation system real time control ability. Numerical simulation results indicate that the proposed semi-active control system produced much better isolation performance than a passive system.

5 REFERENCES

Anakwa W.K.N., Thomas D.R., Jones S.C., Bush J., Green D., Anglin G.W., Rio R., Sheng J., Garrett S., Chen L., 2002, Development and Control of a Prototype Pneumatic Active Suspension System, IEEE Transactions on Education, 45: 43-49.

Choi S.B., Song H.J., Lee H.H., Lim S.C., Kim J.H., Choi H.J., 2003, Vibration control of a passenger vehicle featuring magnetorheological engine mounts, International Journal of Vehicle Design, 33: 2-16.

Choi Y.T., Wereley N.M., Jeon Y.S., 2005, Semi-Active vibration isolation using Magnetorheological isolators, Journal of Aircraft, 42: 1244-1251.

Cronje J.M., Heyns P.S., Theron N.J., Loveday P.W., 2005, Development of a variable stiffness and damping tunable vibration isolator, Journal of Vibration and Control 11: 381-396.

Daley S., Hatonen J., Owens D.H., 2006, Active vibration isolation in a "smart spring" mountl using a repetitive control approach, Control Engineering Practice 14: 991–997.

Duan Y.F., Ni Y.Q., Ko J.M., 2006, Cable vibration control using magnetorheological dampers, Journal of Intelligent Material Systems and Structures, 17: 321-325.

Kobori T., Takahashi M., Nasu T., Niwa N., 1993, Seismic response controlled structure with active variable stiffness system, Earthquake Engineering and Structural Dynamics, 22: 925-941.

Li W.H., Du H., 2003, Design and experimental evaluation of a magnetorheological brake, International Journal of Advanced Manufacturing Technology, 21: 508-515.

Li W.H., Du H., Guo N.Q., 2004, Dynamic behavior of MR suspensions at moderate flux densities, Materials Science & Engineering, A, 371: 9-15.

Nemoto H., active vibration isolation support system, 2006, US patent 7192014 B2.

Ohta K., chida S.U, Miyake T., 2006, vibration isolating mount device, US patent 7111705 B2.

Pnevmatikos N.G., Kallivokas L.F., Gantes C.J., 2004, Feedforward control of active variable stiffness systems for mitigating seismic hazardin structures, Engineering Structures, 26: 471–483.

Spencer B.F., Sain M.K., Carlson J.D., 1998, An experimental study of MR dampers for seismic protection, Smart Materials & Structures, 7: 693-703.

Sun L., Cai X.M., Yang J., 2007, Genetic algorithm-based optimum vehicle suspension design using minimum dynamic pavement load as a design criterion, Journal of Sound and Vibration 301: 18-27.

Sun Y.S., Wang W.H., Wu J.H., Mao Y.C., 2006, Vibration isolation Device, US patent 7114692 B2.

Wang X., 2002, Nonlinear behavior of Magnetorheological (MR) fluids and MR dampers for vibration control of structural systems, PhD thesis, University of Nevada, Reno.

Zhu W.H., Tryggvason B., Piedboeuf J.C., 2006, On active acceleration control of vibration isolation systems, Control Engineering Practice 14: 863–873.